

Toward performance-diverse small-molecule libraries for cell-based phenotypic screening using multiplexed high-dimensional profiling

Mathias J. Wawer^a, Kejie Li^a, Sigrun M. Gustafsdottir^a, Vebjorn Ljosa^b, Nicole E. Bodycombe^a, Melissa A. Marton^c, Katherine L. Sokolnicki^b, Mark-Anthony Bray^b, Melissa M. Kemp^a, Ellen Winchester^c, Bradley Taylor^c, George B. Grant^c, C. Suk-Yee Hon^a, Jeremy R. Duvall^d, J. Anthony Wilson^a, Joshua A. Bittker^d, Vlado Dančík^{a,e}, Rajiv Narayan^f, Aravind Subramanian^f, Wendy Winckler^c, Todd R. Golub^f, Anne E. Carpenter^b, Alykhan F. Shamji^a, Stuart L. Schreiber^{a,1}, and Paul A. Clemons^{a,1}

^aCenter for the Science of Therapeutics, ^bImaging Platform, ^cGenomics Platform, ^dCenter for the Development of Therapeutics, and ^fCancer Program, Broad Institute, Cambridge, MA 02142; and ^eMathematical Institute of the Slovak Academy of Sciences, 04001 Košice, Slovak Republic

Contributed by Stuart L. Schreiber, June 13, 2014 (sent for review April 7, 2014)

High-throughput screening has become a mainstay of small-molecule probe and early drug discovery. The question of how to build and evolve efficient screening collections systematically for cell-based and biochemical screening is still unresolved. It is often assumed that chemical structure diversity leads to diverse biological performance of a library. Here, we confirm earlier results showing that this inference is not always valid and suggest instead using biological measurement diversity derived from multiplexed profiling in the construction of libraries with diverse assay performance patterns for cell-based screens. Rather than using results from tens or hundreds of completed assays, which is resource intensive and not easily extensible, we use high-dimensional image-based cell morphology and gene expression profiles. We piloted this approach using over 30,000 compounds. We show that small-molecule profiling can be used to select compound sets with high rates of activity and diverse biological performance.

chemical diversity | biological performance diversity | biological activity | chemical similarity

Profilng small molecules based on multiple biological activity measurements can illuminate mechanisms of action by comparing profiles with compounds whose mechanisms of action are known (1–5). Here, we describe a previously unidentified use of small-molecule profiling—enabling the creation of activity-enriched and performance-diverse compound libraries for small-molecule probe and drug discovery.

Biochemical and cell-based high-throughput screening (HTS) is routinely used to discover novel bioactive molecules through unbiased testing of up to several million compounds per screen (6). However, despite ongoing advances in throughput, compound libraries will always represent only a small fraction of all relevant compounds theoretically accessible through chemical synthesis (a concept often referred to as “chemical space”) (7). Library composition therefore presents a strong source of bias and potential limitation for any screening endeavor.

There is little dissent about the notion that a good screening collection should yield many high-quality hits for a wide range of biological targets or phenotypes. In other words, it should be enriched for bioactive compounds and have high biological performance diversity. A high percentage of compounds lacking any activity will contribute to high cost and low performance of a high-throughput screen. A practical example is a compound collection containing a high percentage of compounds that fail to penetrate cell membranes—such a library will be unlikely to perform effectively in a cell-based HTS exploring an intracellular process. Similarly, a screening collection of compounds with highly redundant biological activities will be less efficient than an equally sized library with diverse performance (Fig. 1). A

systematic path to reach these goals, however, remains elusive. One common practice is analyzing structural features of compounds to maximize chemical structural diversity. However, the success of this approach requires that similarities and differences in chemical structure be reflected in biological activities—a similarity principle known to have limited applicability (8, 9). Other common strategies include controlling physicochemical parameters (10), exploiting natural selection by sourcing natural products, or relying on natural product-like analogs (11).

None of these approaches measure biological activity or performance diversity directly. However, high-granularity measurements of biological performance diversity have recently come within reach through inexpensive high-throughput profiling methods. Especially attractive are unbiased, high-dimensional measurements relying on “universal languages” such as gene expression or cell morphology, performed as multiplexed measurements in a single well. We hypothesize that these methods provide a means to maximize biological activity and performance diversity of a screening collection by “filtering” a starting collection of

Significance

A large compound screening collection is usually constructed to be tested in many distinct assays, each one designed to find modulators of a different biological process. However, it is generally not known to what extent a compound collection actually contains molecules with distinct biological effects (or even any effect) until it has been tested for a couple of years. This study explores a cost-effective way of rapidly assessing the biological performance diversity of a screening collection in a single assay. By simultaneously measuring a large number of cellular features, unbiased profiling assays can distinguish compound effects with high resolution and thus measure performance diversity. We show that this approach could be used as a filtering strategy to build effective screening collections.

Author contributions: M.J.W., S.M.G., C.S.-Y.H., J.A.B., T.R.G., A.E.C., A.F.S., S.L.S., and P.A.C. designed research; S.M.G., V.L., M.A.M., K.L.S., M.M.K., E.W., B.T., G.B.G., J.R.D., J.A.W., J.A.B., and W.W. performed research; M.J.W., K.L., V.L., N.E.B., M.A.M., M.-A.B., E.W., V.D., R.N., A.S., A.E.C., A.F.S., S.L.S., and P.A.C. analyzed data; M.J.W., S.L.S., and P.A.C. wrote the paper; and C.S.-Y.H. served as a Project Manager.

The authors declare no conflict of interest.

Freely available online through the PNAS open access option.

Data deposition: Compound structures, profiling data, and assay hit counts reported in this paper are publicly available at www.broadinstitute.org/mlpcn/data/Broad.PNAS2014.ProfilingData.zip. The majority of assay results are publicly accessible through ChemBank and PubChem/BARD (Datasets S1 and S2).

¹To whom correspondence may be addressed. Email: stuart_schreiber@harvard.edu or pclemons@broadinstitute.org.

This article contains supporting information online at www.pnas.org/lookup/suppl/doi:10.1073/pnas.1410933111/-DCSupplemental.

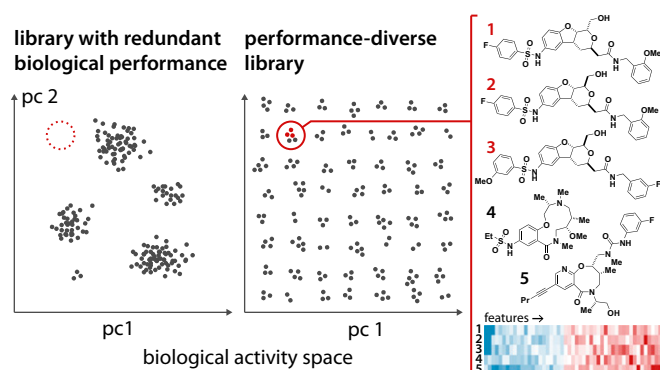


Fig. 1. A performance-diverse library should cover bioactivity space with uniformly distributed sets of compounds. Shown are schematic distributions of performance-redundant (*Left*) and performance-diverse (*Right*) libraries of equal size in a hypothetical 2D projection of a high-dimensional biological activity space (pc: principal component). The diverse library probes a wider bioactivity space with compounds of diverse biological function. For example, the region highlighted in red is unpopulated in the redundant library (*Left*). In the performance-diverse library (*Right*), it would be populated by a small group of compounds having similar performance characteristics. To illustrate, the five compounds on the right are a subset of the 19,164 diversity-oriented synthesis-derived compounds (DOS). They represent a cluster of 14 compounds that were found to elicit a gene expression signature not seen among other members of the DOS set or the known bioactive molecules and confirmed screening hits (BIO). The structures of the five compounds illustrate that not all of the members of a subset need to be structurally similar. However, having clear SAR among biologically similar compounds (structures 1–3) can greatly increase confidence in identified hits and allow rapid follow-up studies.

candidate compounds, ideally a diverse set from natural and synthetic sources. This strategy can help avoid screening many inactive compounds or sets with highly redundant bioactivity.

Due to the novelty of multiplexed profiling methods, this hypothesis has not been tested before. However, the analysis of biological performance and its relationship to chemical structure has previously been undertaken using “parallel” profiles, i.e., compositions of results from independent cell-based or biochemical measurements for a compound that were conducted one at a time. We applied parallel cell-based assay profiling (12, 13) to explore relationships between performance diversity and chemical features such as stereochemistry (14) and skeletons (12). This approach aimed at guiding the creation of effective screening collections for cell-based, phenotypic HTS. We also applied parallel biochemical assay profiling (15) to explore relationships between protein-binding performance diversity and similar chemical features as well as the role of origins of compounds. The latter study addresses the problem of defining effective screening collections for biochemistry-based HTS involving protein binding and activity modulation (for example, enzyme inhibition).

Parallel profiling has further been used to inform compound library design independently of chemical structure considerations. In seminal work, Kauvar et al. (16) Kauvar (17), and Beroza et al. (18) suggested selecting compounds with distinct *in vitro* binding (biochemical) profiles against a panel of reference proteins to avoid “clumps” in bioactivity space. However, thorough evaluations of how these and other selection strategies affect the performance of real-world libraries are rare.

One notable exception is a recent retrospective analysis of the Novartis screening collection (9), showing that library subsets selected for high performance diversity achieve high hit rates in more assays than those selected for high chemical diversity alone. Performance diversity was measured as the number of unique target annotations for a set of compounds. The main drawback of this approach is that large amounts of historical

bioactivity data are required, making it more useful for triaging well-tested collections and less so for informing decisions about novel libraries or library expansion.

We therefore sought to develop a high-throughput and extensible method to specify performance-diverse small-molecule libraries for cell-based screens. To avoid the impracticalities of conducting numerous independent assays on a novel set of small molecules, we chose two recently developed profiling technologies where up to 1,000 measurements can be made from a single well. The methods capture cell morphology (19) and gene expression (20) to characterize complex cell states. Unbiased profiling has been shown to capture the mechanistic details of a wide range of bioactivities (4, 5, 21) and we hypothesized it would assist in defining the composition of performance-diverse small-molecule libraries for cell-based screening. We evaluated the performance of cell morphology and gene expression profiling, using real-world screening data, and show that both methods can be used in the specification of performance-diverse small-molecule libraries for cell-based screens (Fig. 2). Our results also suggest that combining the two methods may offer greater value than either one individually.

Results

We collected cell-morphology profiles from U-2 OS osteosarcoma cells treated with each of 31,770 compounds at a single concentration. Our compound collection comprised 12,606 known bioactive molecules and confirmed screening hits (BIO) as well as 19,164 novel compounds derived from diversity-oriented synthesis (DOS). The DOS set was selected without taking any bioactivity data into account. Changes in cell morphology were measured after 48 h of treatment, using a multiplexed-cytological (MC) “cell-painting” assay (19). Cells were stained with six different fluorescent markers to distinguish cellular compartments and organelles. Automated microscopy and image analysis led to profiles of 812 morphology features (19).

Cell Morphology Profiling Can Be Used to Enrich Libraries for Hits in Phenotypic HTS. An effective library construction strategy should preferentially select compounds that show activity in HTS. It is an open question whether unbiased biological profiling is sensitive and specific enough to infer activity in a range of targeted assays from observing reproducible profiles. We found that sets of compounds showing activity in the MC assay are enriched for HTS hits.

We first determined the set of “hits” for MC profiling, i.e., compounds that induced stable and characteristic morphological changes in U-2 OS cells. We used the multidimensional perturbation value (mp value) described by Hutz et al. (22) to measure compound activity in profiling assays. Compounds were considered active if they significantly differed from DMSO negative controls ($P < 0.05$). As expected, due to the preselection for biological activity in the BIO set only, the hit rate of BIO compounds in our

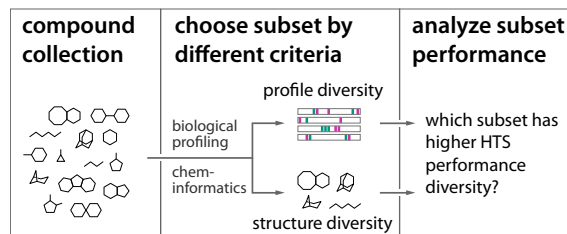


Fig. 2. We compared compound selection criteria based on HTS performance diversity. Starting with a compound collection, we selected diverse subsets by either biological profiling (MC or GE; main text) or chemical structure. We then compared these subsets with respect to their performance diversity across many HTS assays.

MC assay (68.3%) exceeded the hit rate of the DOS set (37.0%; *SI Appendix, Table S1*). Notably, the MC assay was able to identify more than two-thirds of the BIO collection as active. The relatively high hit rates could potentially arise due to statistical significance of effect sizes that are not biologically relevant. If this is of concern, additional constraints can be placed on the activity scores underlying the P -value calculations, as suggested by the authors of the mp-value study (22). For the purpose of this study, we chose to use the standard threshold because we are interested in general statistical trends rather than individual high-confidence hits.

We then analyzed the HTS assay performance of these MC assay hits. Based on HTS data from 96 cell-based screening projects (comprising 178 individual assays and 512 different assay measurements) performed by the Center for the Science of Therapeutics at the Broad Institute, we found that compounds active in our MC assay were significantly enriched for hits in HTS (Fig. 3). We limited our analysis to cell-based HTS assays because the profiling described here depends on testing live cells; profiling is thus used to define optimal libraries for cellular screens. Importantly, these assays cover a variety of fluorescence- and luminescence-based readouts that are dissimilar from our image-based MC assay (*SI Appendix, Tables S2–S4*). Five of these assays (67 measurements; 13%) were based on imaging and 14 assays (14 measurements; 2.7%) used U-2 OS cells. For each compound, we calculated a hit frequency as the fraction of HTS assays in which it achieved a minimum absolute z score of 3 relative to the DMSO control distribution (23). The median HTS hit frequency for compounds active in the MC assay (2.78%) was significantly higher than for all tested compounds (1.96%; one-sided Wilcoxon $P = 4.5 \times 10^{-17}$; Fig. 3A). Likewise, the set of compounds inactive in the MC assay was significantly depleted for HTS hits (median hit frequency = 0%; $P = 1.5 \times 10^{-27}$; Fig. 3A). We conclude that activity in a morphological profiling assay can be used to enrich screening libraries for bioactive compounds. Furthermore, the extent of the difference between treatment and the negative control was associated with the HTS hit frequency. Compounds that showed larger differences and thus stronger activity in the MC assay had larger HTS hit frequencies (Fig. 3B and C). This suggests that multiplexed profiling could provide a way of flagging potentially promiscuous compounds before they appear as false positives in numerous screens.

Compound Sets with Diverse Cell Morphology Profiles Have Diverse Performance in Cell-Based HTS Assays. We next tested whether MC profiling provides a practical approach to creating compound libraries with diverse biological performance for cell-based screens (Fig. 2). We found that selection of compounds with diverse MC profiles led to higher HTS performance diversity than either random selection or selection of diverse chemical structures (Fig. 4).

We first ensured that MC profiles reliably captured similarities and differences in biological performance with high granularity—a prerequisite for selecting diverse bioactivities. Hierarchical clustering of well-annotated BIO compounds based on their MC profiles grouped compounds with similar biological effects together (*SI Appendix, Fig. S1*), confirming results from earlier studies (19, 24).

We then compared different compound selection criteria—MC profile diversity, chemical structure diversity, and random selection—with respect to their ability to select compounds with diverse HTS performance. HTS performance diversity was measured by first constructing an HTS assay profile for each compound, indicating for each assay in which the compound was tested whether it scored significantly positive (encoded as 1), scored significantly negative (−1), or was not a hit (0). Compounds were then clustered based on their HTS profiles and we calculated (i) the absolute number of distinct clusters represented in a compound set and (ii) the set diversity (or effective number of distinct clusters). The set diversity is an information-theoretic measure that takes the distribution of compounds over clusters

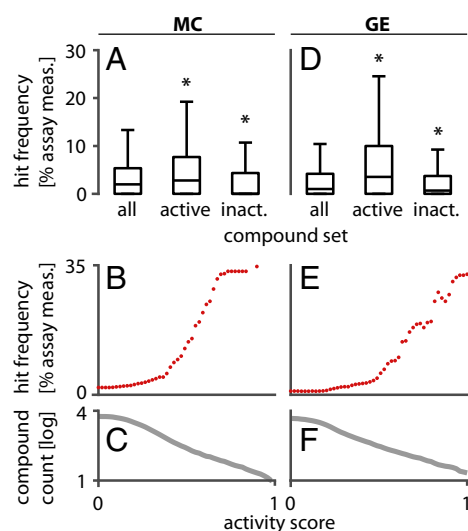


Fig. 3. Sets of compounds that are active in MC and GE profiling are enriched for HTS hits. (A) Boxplots showing the distribution of HTS hit frequencies (HF, fraction of HTS assay measurements in which a compound scored as a hit) for compound sets in the MC study. Compared with all tested compounds, the HF is significantly higher for compounds active in the MC assay [median(HF_{all}) = 1.96%; median(HF_{act}) = 2.78%; one-sided Wilcoxon $P = 4.5 \times 10^{-17}$]. Likewise, the HF is significantly lower for compounds inactive in our MC assay [median(HF_{inact}) = 0.00%, $P = 1.5 \times 10^{-27}$]. (B and C) Compounds with higher activity in the MC assay have higher HF. HF (B) and compound numbers on a \log_{10} scale (C) are plotted for all compounds that exceed a given activity score (*SI Appendix*). (D) Boxplots of HFs for compound sets in the GE study. The set of active compounds for the GE assay is enriched for HTS hits [(D) median(HF_{all}) = 0.99%; median(HF_{act}) = 3.52%; $P = 2.2 \times 10^{-28}$] whereas the set of inactive compounds is depleted for HTS hits [median(HF_{inact}) = 0.67%, $P = 1.0 \times 10^{-4}$]. (E and F) Compounds with higher activity in the GE assay have higher hit frequencies.

into account, rewarding even distributions over clusters and penalizing sets for which a large fraction of compounds fall into only a few clusters (Fig. 4A). In summary, a maximally performance-diverse set in this context would consist of compounds that all have distinct HTS assay profiles. In a set lacking performance diversity, all compounds would have the same profile (Fig. 4A).

We compared the HTS performance diversity of compound sets selected to have (i) diverse MC profiles and (ii) diverse chemical structures (CS) to randomly selected compound sets (RND). To allow a direct comparison, we applied all three selection methods to the same set of compounds. This “test collection” consisted of all unique compounds in our experiment for which MC profiles with reliable signal were available (mp-value $P < 0.05$) and that were tested in at least 15 HTS assays to calculate meaningful assay profiles. We further included only compounds that were a hit in at least one HTS assay to avoid having a large pool of all-zero HTS profiles considered performance redundant only because the compounds had not been tested in enough assays. If a compound had been tested multiple times, we kept only the instance with the highest activity score to exclude trivial redundancy due to identical treatments. In all, 7,154 compounds fulfilled these selection criteria. At baseline, this test collection covered 665 distinct assay profile clusters and achieved 23.9% of the maximum theoretical diversity (100% diversity would be achieved if each cluster were represented by the same number of compounds). This result indicates that a considerable number of compounds fall into only a few clusters and thus have redundant biological performance, providing a good test case for our method.

We selected subsets ranging from $n = 1$ to $n = 7,154$ compounds, using MC, CS, or RND as a selection criterion (*SI Appendix,*

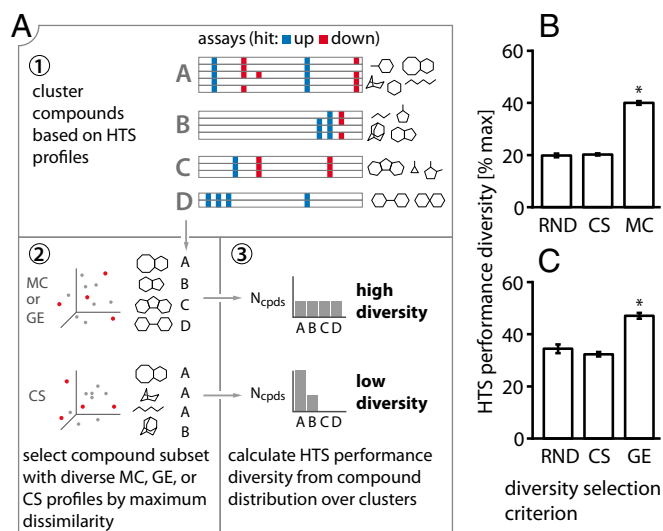


Fig. 4. Biological profiling can support the selection of performance-diverse compound collections. (A) Conceptual outline of diversity experiment. We first clustered a test collection of compounds based on their HTS profiles (step 1). From the same test collection, we selected compound subsets based on MC (or GE) diversity and CS diversity, using a maximum dissimilarity strategy (step 2). The compounds in each subset were annotated with the HTS clusters determined in step 1. Based on the distribution of compounds over clusters, we then determined for each subset the HTS performance diversity (step 3). A subset with high performance diversity would contain compounds that are equally spread over many clusters. A subset with low diversity would contain a large fraction of compounds that fall into only a few HTS clusters. (B and C) Results for the subset size that achieved the highest HTS performance diversity across all selection methods, using a random compound selection (RND) as baseline (results on all subset sizes in *SI Appendix, Fig. S2*). Asterisks indicate significant diversity increases over RND. (B) Results for the MC study (test-collection size, $n = 7,154$ compounds; subset size, $n_{\text{sub}} = 1,399$). Selecting compounds with diverse MC profiles led to significantly higher HTS performance diversity than random selection (Wilcoxon rank-sum $P = 2.9 \times 10^{-165}$). (C) Results for the GE study ($n = 1,363$; $n_{\text{sub}} = 463$). GE diversity selection led to higher HTS performance diversity than random selection ($P = 2.9 \times 10^{-165}$). For both the MC and the GE test collection, selection based on chemical structure diversity did not notably increase HTS performance diversity over the random control.

Fig. S24). MC diversity selection led to the highest overall HTS performance diversity, significantly improving over the baseline of all compounds in the test collection while selecting only less than a fifth of them (1,399 compounds achieve 40.0% diversity, covering 71.9% of all clusters; *Fig. 4B* and *SI Appendix, Figs. S24* and *S34*). This value significantly exceeded the HTS performance diversity of sets selected randomly (19.8%; 46.6% of clusters; one-sided Wilcoxon $P = 2.9 \times 10^{-165}$). By contrast, the traditionally applied CS-diversity-based selection did not lead to notably higher performance diversity than random selection (20.2%; 47.9% of clusters; *Fig. 4B* and *SI Appendix, Figs. S24* and *S34*). This result supports our hypothesis that single-well biological profiling can be used to select compound sets with diverse HTS assay performance patterns.

Technically, the diversity measure quantifies the effective number of clusters (groups of compounds having similar HTS performance) in a library, i.e., how many clusters with an equal number of members would be needed to achieve the same average cluster variety in a sample drawn from that library. In practice, this means that if the diversity is low, a few clusters will be highly overrepresented and can easily dominate the top of screening hit lists, especially if they are associated with relatively nonspecific biological effects (e.g., toxicity). Random selection conserves the relative representation of each cluster in the full dataset; therefore, a reduction in compound numbers using

random selection (or the similarly performing selection based on chemical structure) will lead to a loss of small clusters, i.e., rare HTS performance patterns. Our data suggest that profile-based selection could by contrast “compress” the HTS performance information per tested compound in the library by a factor of 8 (40% with one-fifth of the library vs. 23.9% for all compounds), while retaining most of the unique HTS performance patterns (71.9%). Relative to the random and HTS structure-based selection, this represents a twofold increase in diversity and a 54% increase in unique HTS performance patterns.

Gene Expression-Based Selection Can Identify Sets of Compounds Enriched for HTS Hits and Diverse HTS Performance. We repeated our analysis with gene expression (GE) profiles collected after 6 h of treatment. Using cost-effective ligation-mediated amplification and bead-based detection (20), we measured the expression levels of 977 protein-coding RNA transcripts per sample. The transcripts were selected to be largely uncorrelated and capture about 80% of the similarity information of genome-wide expression profiles (~22,000 transcripts; <http://linccscloud.org/the-landmark-genes/>). We collected GE profiles for 17,553 DOS and 4,199 BIO compounds, the majority of which were also part of our MC profiling experiment (*SI Appendix, Tables S1* and *S5*). On each plate, we included a set of positive control (POS) compounds that have been shown to elicit strong gene expression changes across different cell lines (4).

Almost all POS compounds were active in the GE assay (96.6%; *SI Appendix, Table S1*). The GE assay “hit” rates for bioactive compounds (39.0%) and DOS compounds (11.0%) were lower than those of the MC assay (*SI Appendix, Table S1*). A possible explanation is that we measured compounds in triplicate in the GE assay and in quadruplicate in the MC assay and were thus able to detect smaller effect sizes in the MC assay. Furthermore, the cells in the MC study were exposed to compounds longer than in the GE study (48 h vs. 6 h).

Compounds active in our GE assay were significantly enriched for hits in cell-based HTS (*Fig. 3D*), resembling the results from our MC study. The median HTS hit frequency for compounds active in the GE assay (3.52%) was significantly higher than for all tested compounds (0.99%; one-sided Wilcoxon $P = 2.2 \times 10^{-28}$, *Fig. 3D*). The set of compounds inactive in profiling assays was significantly depleted for HTS hits (median hit frequency = 0.67%; $P = 1.0 \times 10^{-4}$; *Fig. 3D*). As in the MC study, compounds that showed larger profile differences from DMSO negative controls and thus stronger activity in the GE assay had larger HTS hit frequencies (*Fig. 3E* and *F*). We conclude that GE profiling can inform the selection of collections enriched for active compounds and possibly guide the selection of compounds based on their expected promiscuity in HTS assays.

We repeated the diversity selection study, using GE profiles. When clustered based on GE profiles, compounds formed groups with related mechanisms of action (*SI Appendix, Fig. S4*). We then selected a compound subset with diverse GE profiles or CS and compared its HTS performance diversity to a randomly selected subset (RND; *Fig. 4A*). Analogous to the MC study, we selected a GE test collection of 1,363 unique compounds, which at baseline achieved 41.5% maximum theoretical diversity and covered 232 distinct clusters. We observed similar results to those of the MC study (*Fig. 4C* and *SI Appendix, Figs. S2B* and *S3B*). By selecting about a third of the test collection (463 compounds) GE profile diversity selection led to the overall highest HTS diversity (47%; 73.2% of clusters), which significantly exceeded results for the random control selection (34.4%; 59.7% of clusters; one-sided Wilcoxon $P = 2.9 \times 10^{-165}$). CS diversity did not lead to higher diversity than random selection (32.2%; 59.3% of clusters). We conclude that GE profiling can be used to select compound sets with diverse HTS performance.

Cell Morphology and Gene Expression Profilings Are Not Redundant.

The hits identified in the MC (48-h treatment) and GE assays (6-h treatment) overlap only partially (Fig. 5*A*). However, the hit sets of MC and GE are also not independent (Fisher's exact test, $P = 3.70 \times 10^{-94}$; Fig. 5*A* and *SI Appendix, Table S5*), indicating that a compound active in one profiling assay is more likely to also be active in the other (compared with the baseline probability of being active). When separated by compound class, DOS compounds showed significant overlap, again indicating that the activity in both assays is not independent. Because many of the bioactives tested in both assays scored as "hits" (MC, 74%; GE, 38%; *SI Appendix, Table S5*), the overlap for the BIO set is not significant (a large overlap is expected by chance if a large fraction of the compounds are active in either assay).

The overlapping hits for both assays are enriched for compounds that scored as positives with a high frequency in cell-based HTS (Fig. 5*B* and *SI Appendix, Fig. S5*). Many of these compounds are known to induce strong cellular responses (e.g., cytotoxic and cytostatic agents; *SI Appendix, Table S6*) and are thus expected to give a strong signal in most cell-based profiling methods. An interesting question that originates from this result is therefore whether the hits identified in imaging and gene expression profiling assays will converge if profiling assay sensitivity and specificity were further optimized or if some bioactivities—due to mechanistic differences—can be detected only in one of the assays. The parameters used for this study (one cell line and different treatment times for MC and GE) limit our ability to provide an answer to this question. However, within the limitations of currently available methods, our data suggest that orthogonal profiling techniques could capture a significantly wider range of bioactivities than either method alone (Fig. 5*A*).

When compared directly on the set of compounds tested in both assays, diversity selection using both MC and GE profiles led to increased HTS performance diversity over random selection, with MC performing better than GE (Fig. 5*C* and *SI Appendix, Figs. S6* and *S7*). Again, using chemical structure diversity as a selection

criterion did not significantly improve HTS performance diversity over random selection.

Discussion

We conclude this study by suggesting the use of multiplexed small-molecule profiling as a strategy to construct performance-diverse libraries for cell-based screens. We have shown that single-well high-throughput cell morphology and gene expression profiling can be used to select compound sets that are highly enriched for compounds that score as HTS hits in cell-based assays without using prior knowledge of the outcomes of those HTS assays. Furthermore, we can exploit the ability of cell morphology and gene expression profiling to group compounds by their mechanism of action to support creation of a performance-diverse compound library. Existing collections can be triaged to reduce existing redundancy of biological performance, and prospective library extension and evolution can be achieved. This method is a powerful partner for short and modular diversity-oriented syntheses, where the initial focus can be on diverse structures computed to have desirable physical and chemical properties (for example, solubility and medicinal chemistry tractability). As we show here, compounds can then be filtered for their performance diversity before entering into a collection optimized for cell-based screens.

Optimally, a library should contain a few compounds for each identified profile type that each differ slightly in their biological performance (Fig. 1). This strategy will help to increase confidence in identified hits in cases where the gene expression and cell morphology features associated with a group of compounds track with their performance in an HTS assay. If, in addition, such biologically similar compounds have similar chemical structures, these allow for easy validation and follow-up through structure–activity relationship (SAR) studies around an identified response (25). However, there is also value in compounds with similar biological performance but dissimilar structure (e.g., compounds 1–3 vs. compounds 4 and 5 in Fig. 1). Besides providing different chemical starting points, observing the same HTS performance for such compounds is even more indicative of related mechanisms of action, as they do not share a structural similarity that could lead to screening artifacts. The latter strategy represents a translation of the concept of SAR analog series from chemical to biological space; i.e., it does not rely on a chemical structure similarity principle.

The extent of improvement over the full library for subsets selected based on chemical diversity depends on many parameters (e.g., redundancy of the library, assay selection, resolution of the HTS data), making it difficult to quantify without prospective analyses on different libraries and assays. Although 40–50% diversity as observed in our studies appears to leave much room for improvement, 100% is a theoretical maximum that is difficult to achieve in practice. This is especially true because we use HTS data as our standard, which is often noisy and likely biased due to the specific assay selection. As a pilot study for testing our results prospectively, we have therefore plated a performance-diverse compound collection, selected using the principles described in this study. We have started to evaluate this collection in cell-based screens.

With an ongoing reduction of both costs and technological hurdles associated with performing multiplexed assays, we anticipate an increasing adoption of high-dimensional profiling assays. This would allow our method to be readily applicable to novel screening collections. Automatic microscopes used for imaging assays are already available at many screening centers. The Luminex technology used for the GE assay is a versatile assay system that is used for various purposes by many laboratories. In addition, ongoing developments in other gene expression measurement technologies (e.g., RNAseq) will similarly simplify large-scale gene expression analyses.

Our results show that different biological profiling methods and assay conditions currently capture different hit sets, possibly including compounds with distinct mechanisms of action. As novel

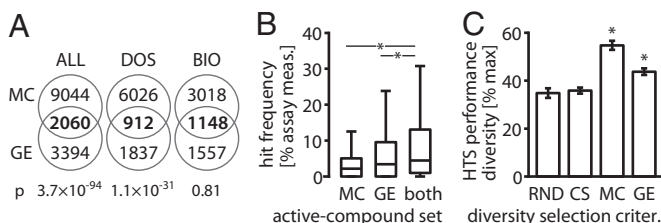


Fig. 5. MC and GE profiling have overlapping yet distinct hit sets. (A) Venn diagrams of the MC and GE hit sets. Although the majority of compounds are identified by only one of the methods, low P values (Fisher's exact test) indicate a nonrandom overlap between two hit sets. Both MC and GE identify a large fraction of the BIO collection as hits; thus even high overlap is not significant (*SI Appendix, Table S5*). (B) Boxplots of HTS hit frequencies (HF, defined in Fig. 3) for active compounds tested in both the MC and the GE study. MC, hits identified based on cell-morphology profiles; GE, hits identified based on gene expression profiles; both, hits identified by both MC and GE. The intersection of the sets of active compounds from the MC and GE assay shows even stronger enrichment for compounds with high HF [median(HF_{both}) = 4.41%] than either set of actives alone [median(HF_{MC}) = 2.14%; one-sided Wilcoxon $P_{MC} = 1.4 \times 10^{-14}$; median(HF_{GE}) = 3.39%; $P_{GE} = 1.9 \times 10^{-3}$]. This indicates that the MC and GE assays tend to agree on compounds that are active in multiple HTS assays and possibly even promiscuous (*SI Appendix, Table S6*). Asterisks indicate significant HF increases. (C) When direct comparison was made on the intersection of the MC and GE test collections ($n = 904$), we observed higher HTS performance diversity than random selection for selection based on both MC (Wilcoxon $P = 2.9 \times 10^{-165}$) and GE profiles ($P = 7.1 \times 10^{-165}$) when selecting about a third of the test collection ($n_{sub} = 320$). Asterisks indicate a significant diversity increase over RND.

profiling methods become suitable for HTS formats, they should be evaluated, using a diverse set of cell lines (or strains, in the case of microbial therapeutics discovery) and assay parameters, to cover a large fraction of the theoretically possible biological measurement space and to enable construction of transformative screening collections for cell-based phenotypic screens. Likewise, the development of biochemical profiling methods should enable construction of effective screening collections for protein-binding and biochemical activity-modulation screens (26).

Materials and Methods

For details, see *SI Appendix*.

MC Morphology Profiles. We followed the protocol published by Gustafsdottir et al. (19) After compound treatment (48 h), we stained the cells for nucleus (Hoechst 33342), endoplasmic reticulum (Con A/AlexaFluor488 conjugate), nucleoli (SYTO 14 green fluorescent nucleic acid stain), Golgi apparatus, and plasma membrane (wheat germ agglutinin/AlexaFluor594 conjugate, WGA), F-actin (phalloidin/AlexaFluor594 conjugate), and mitochondria (Mito-Tracker Deep Red). Morphological features for each cell were obtained through subsequent automatic image capture and analysis.

GE Profiles. We followed the protocol published by Peck et al. (20). After compound treatment (6 h), cells were lysed and expression levels of 977 transcripts quantified using ligation-mediated amplification and Luminex microsphere-based detection.

HTS Hit Frequency and Assay Profiles. Screening results were assembled from an internal Broad Institute database. However, the majority of assays have been published in ChemBank or PubChem/BARD (*Datasets S1 and S2*). We calculated D scores (27) for each assay result to make them comparable across individual assays. For hit-frequency calculations, we used a hit-calling threshold of 3σ (relative to DMSO control), which corresponds to an absolute D score of 3. We chose 35 assays as the lower threshold of performed assay measurements per compound to achieve a probability of more than 50% of being a hit in at least one assay by assuming a true hit rate of 2% per assay. For HTS performance diversity calculations, we discretized result values in three bins ($-1, 0, 1$), using a two-sided activity threshold of 2.5%. We used a lower threshold than for hit calling because the result values were combined into profiles that were exclusively used in similarity calculations. In addition to the denoising effect of considering multiple measurements, capturing weakly active compounds is more important for profile similarity

than for overall hit frequency calculations. Accordingly, the minimum number of assay measurements was decreased to 15.

Diversity Selection. From a set of n compounds, we selected series of diverse compound subsets $S_i, i \in [1, n]$, based on MC profiles, GE profiles, and extended-connectivity fingerprints (ECFP4), using a maximum dissimilarity strategy. A random compound was chosen as the starting set S_1 . To create S_{i+1} , we iteratively added the compound that was most dissimilar to its closest neighbor in S_i until no compounds were left to add (full set S_n). This selection process was repeated 500 times, each time with a random starting compound. Dissimilarity for GE and MC profiles was calculated as pairwise correlation distance ($1 - \text{Pearson correlation coefficient}$) between profiles. Chemical dissimilarity was measured using Jaccard distance (28) on stereochemistry-aware ECFP4 fingerprints (ECFP4#S) (29).

HTS Performance Diversity. We hierarchically clustered compounds based on their HTS assay profiles, using weighted-average linkage applied to Jaccard distances. The resulting dendrogram was cut at a distance of 0.8 to obtain final cluster assignments. We calculated the performance diversity for a set of compounds C as the effective number of HTS clusters using the true diversity D (30):

$$D = \exp\left(-\sum_{i=1}^R p_i \ln p_i\right) = e^H.$$

Here, R is the number of distinct clusters in C , p_i is the fraction of compounds in C that are members of cluster i , and H is the Shannon entropy (30).

ACKNOWLEDGMENTS. The authors acknowledge technical assistance in gene expression profiling from the Broad Institute Genomics Platform. We also thank the compound management and screening groups of the Broad Institute Chemical Biology Platform, especially Tom Hasaka for assistance with automated microscopy. We thank David Lahr, Jacob Asiedu, and Patrick Faloon for assistance with annotating HTS assays. The authors are extremely grateful to Dr. Yan Feng of Novartis Institutes of Biomedical Research, whose thoughtful comments during the review process led directly to our adoption of normalized mp values to call profile hits, substantially improving our results. This work was supported by the National Institutes of Health as part of the Molecular Libraries Probe Production Centers Network program (U54 HG005032 awarded to S.L.S.) and the Library of Integrated Network-based Cellular Signatures program (U54 HG006093, large-scale gene expression analysis of cellular states, awarded to A.S. and T.R.G.), the National Institute of General Medical Sciences (P50-GM069721 awarded to S.L.S.) as part of the Center of Excellence for Chemical Methodology and Library Development, and the National Science Foundation (CAREER DBI 1148823 awarded to A.E.C.). S.L.S. and T.R.G. are investigators at the Howard Hughes Medical Institute.

- Bai RL, et al. (1991) Halichondrin B and homohalichondrin B, marine natural products binding in the vinca domain of tubulin. Discovery of tubulin-based mechanism of action by analysis of differential cytotoxicity data. *J Biol Chem* 266(24):15882–15889.
- Paul KD, Lin CM, Malspeis L, Hamel E (1992) Identification of novel antimetabolic agents acting at the tubulin level by computer-assisted evaluation of differential cytotoxicity data. *Cancer Res* 52(14):3892–3900.
- Hughes TR, et al. (2000) Functional discovery via a compendium of expression profiles. *Cell* 102(1):109–126.
- Lamb J, et al. (2006) The Connectivity Map: Using gene-expression signatures to connect small molecules, genes, and disease. *Science* 313(5795):1929–1935.
- Feng Y, Mitchison TJ, Bender A, Young DW, Tallarico JA (2009) Multi-parameter phenotypic profiling: Using cellular effects to characterize small-molecule compounds. *Nat Rev Drug Discov* 8(7):567–578.
- Macarron R, et al. (2011) Impact of high-throughput screening in biomedical research. *Nat Rev Drug Discov* 10(3):188–195.
- Reymond JL, Awale M (2012) Exploring chemical space for drug discovery using the chemical universe database. *ACS Chem Neurosci* 3(9):649–657.
- Maggiore GM (2006) On outliers and activity cliffs—why QSAR often disappoints. *J Chem Inf Model* 46(4):1535.
- Petrone PM, et al. (2013) Biodiversity of small molecules—a new perspective in screening set selection. *Drug Discov Today* 18(13–14):674–680.
- Leeson PD, Springthorpe B (2007) The influence of drug-like concepts on decision-making in medicinal chemistry. *Nat Rev Drug Discov* 6(11):881–890.
- Wetzel S, Bon RS, Kumar K, Waldmann H (2011) Biology-oriented synthesis. *Angew Chem Int Ed Engl* 50(46):10800–10826.
- Kim YK, et al. (2004) Relationship of stereochemical and skeletal diversity of small molecules to cellular measurement space. *J Am Chem Soc* 126(45):14740–14745.
- Wagner BK, Clemons PA (2009) Connecting synthetic chemistry decisions to cell and genome biology using small-molecule phenotypic profiling. *Curr Opin Chem Biol* 13(5–6):539–548.
- Tanikawa T, et al. (2009) Using biological performance similarity to inform disaccharide library design. *J Am Chem Soc* 131(14):5075–5083.
- Clemons PA, et al. (2011) Quantifying structure and performance diversity for sets of small molecules comprising small-molecule screening collections. *Proc Natl Acad Sci USA* 108(17):6817–6822.
- Kauvar LM, et al. (1995) Predicting ligand binding to proteins by affinity fingerprinting. *Chem Biol* 2(2):107–118.
- Kauvar LM (1995) Affinity fingerprinting. *Biotechnology* 13(9):965–966.
- Beroza P, Villar HO, Wick MM, Martin GR (2002) Chemoproteomics as a basis for post-genomic drug discovery. *Drug Discov Today* 7(15):807–814.
- Gustafsdottir SM, et al. (2013) Multiplex cytological profiling assay to measure diverse cellular states. *PLoS ONE* 8(12):e80999.
- Peck D, et al. (2006) A method for high-throughput gene expression signature analysis. *Genome Biol* 7(7):R61.
- Young DW, et al. (2008) Integrating high-content screening and ligand-target prediction to identify mechanism of action. *Nat Chem Biol* 4(1):59–68.
- Hutz JE, et al. (2013) The multidimensional perturbation value: A single metric to measure similarity and activity of treatments in high-throughput multidimensional screens. *J Biomol Screen* 18(4):367–377.
- Seiler KP, et al. (2008) ChemBank: A small-molecule screening and cheminformatics resource database. *Nucleic Acids Res* 36(Database issue):D351–D359.
- Ljosa V, et al. (2013) Comparison of methods for image-based profiling of cellular morphological responses to small-molecule treatment. *J Biomol Screen* 18(10):1321–1329.
- Wawer MJ, et al. (2014) Automated structure-activity relationship mining: Connecting chemical structure to biological profiles. *J Biomol Screen* 19(5):738–748.
- Clemons PA, et al. (2010) Small molecules of different origins have distinct distributions of structural complexity that correlate with protein-binding profiles. *Proc Natl Acad Sci USA* 107(44):18787–18792.
- Dančik V, et al. (2014) Connecting small molecules with similar assay performance profiles leads to new biological hypotheses. *J Biomol Screen* 19(5):771–781.
- Jaccard P (1902) Lois de distribution florale dans la zone alpine. *Bull Soc Vaud Sci Nat* 38(144):69–130.
- Rogers D, Hahn M (2010) Extended-connectivity fingerprints. *J Chem Inf Model* 50(5):742–754.
- Hill MO (1973) Diversity and evenness: A unifying notation and its consequences. *Ecology* 54(2):427–432.

Supporting Information

Towards performance-diverse small-molecule libraries for cell-based phenotypic screening using multiplexed high-dimensional profiling

Mathias J. Wawer^a, Kejie Li^a, Sigrun M. Gustafsdottir^a, Vebjorn Ljosa^b, Nicole E. Bodycombe^a, Melissa A. Marton^c, Katherine L. Sokolnicki^b, Mark-Anthony Bray^b, Melissa M. Kemp^a, Ellen Winchester^c, Bradley Taylor^c, George B. Grant^c, C. Suk-Yee Hon^a, Jeremy R. Duvall^d, J. Anthony Wilson^a, Joshua A. Bittker^d, Vlado Dančík^{a,e}, Rajiv Narayan^f, Aravind Subramanian^f, Wendy Winckler^c, Todd R. Golub^f, Anne E. Carpenter^b, Alykhan F. Shamji^a, Stuart L. Schreiber^{a*}, Paul A. Clemons^{a*}

^aCenter for the Science of Therapeutics, ^bImaging Platform, Broad Institute, ^cGenomics Platform, Broad Institute, ^dCenter for the Development of Therapeutics, and ^eCancer Program, Broad Institute, 7 Cambridge Center, Cambridge, MA 02142, USA; and ^fMathematical Institute of the Slovak Academy of Sciences, 04001 Košice, Slovak Republic

*Corresponding authors

Stuart L. Schreiber, stuart_schreiber@harvard.edu
Paul A. Clemons, pclemons@broadinstitute.org

Supporting Materials and Methods

Compound selection

The DOS compound collection represents a structurally diverse subset of 19,637 compounds selected from 23 DOS libraries. (1-8) These libraries were synthesized using a build-couple-pair strategy (9) to combine simple chiral building blocks into diverse and complex compounds. (10) Each library is built around a common chiral core by varying side chains and the configurations of core stereocenters. For most compounds, all stereoisomers were synthesized.

For each library, we determined the set of unique stereochemical “parent” structures, *i.e.*, structures with unspecified stereochemistry. We exposed these sets to a maximum dissimilarity selection algorithm using Tanimoto similarity (11) on ECFP4 fingerprints (12) for each chiral core separately. In collaboration with the Broad Institute Discovery Chemistry and Compound Management teams, we determined the desired proportion of compounds from each library, and for those stereochemical parents selected, included all stereoisomers with physical samples available.

The BIO collection comprised three different compound sets. First, we included 2,222 drugs, natural products, and small-molecule probes that are part of the Broad Institute known bioactive compound collection. The collection contains structurally diverse compounds across a wide range of biological activities with known targets for many compounds. Second, we extended this set by selecting 274 hits or structural analogs from various probe-development projects sponsored by the Molecular Libraries Program (MLP). Third, we selected 10,162 compounds from the Molecular Libraries Small Molecule Repository (MLSMR). Assay activity data from Molecular Libraries Probe Production Centers (MLPCN) screening centers reported as percent activity were retrieved from PubChem (<http://pubchem.ncbi.nlm.nih.gov/>). To include bioactive but not promiscuous compounds, we kept only compounds that had been tested in >50% of all assays (unique AIDs) performed on the MLSMR collection and that were hits in at least 2 but fewer than 10% of assays tested. Compounds were selected to cover many different chemical structures and biological activities.

Differences between the total compound numbers reported here and those in Table S1 are due to quality control filters on GE and MC experimental data.

Gene-expression assay

We followed the protocol published by Peck et al. (13) Briefly, we seeded 3,500 U-2 OS cells (ATCC, cat. no. HTB-96) per well in 384-well plates. After 24h of incubation at 37°C, compounds were added to the cells, followed by another 6h of incubation. Treatments were carried out in triplicates. The cells were then lysed and lysates transferred to oligo-dT plates to capture mRNAs. We reverse-transcribed mRNA and amplified cDNA via polymerase chain reaction (PCR). We annealed the cDNA to a mix of upstream/downstream probe pairs, each of which was designed to be specific for one of 977 transcripts. Each upstream probe consisted of a universal 20-nucleotide (nt) primer site

(complementary to T7 primer), a unique 24-nt barcode sequence, and a 24-nt sequence designed to bind to the 3'-end of one specific transcript. Downstream probes were designed to anneal contiguous to their corresponding upstream probe on the transcript. They consist of a 5'-phosphorylated 20-nt transcript-specific sequence and a 20-nt universal primer site (T3). Any unbound probes were removed after the annealing step. Only upstream and downstream probes that bound next to each other on a transcript cDNA molecule were ligated in the next step and then amplified by PCR using T3 and 5'-biotinylated T7 primers. We added these amplicons to a mix of color-coded Luminex microspheres, each of which carried capture probes complementary to one of the barcode sequences in the amplicons. Streptavidin-phycoerythrin was added to add fluorescent markers to the biotinylated amplicons. The number of captured amplicons was then quantified by flow cytometry measuring phycoerythrin fluorescence. Transcript identity was identified by microsphere color.

Gene-expression: cell plating and compound treatment

1. U-2 OS cells (ATCC, cat. no. HTB-96)
2. 384 well plates (Corning, cat. no. 3712)
3. culture medium
 - DMEM (Fisher Scientific, cat.no. MT10017CV)
 - 10%FBS (Life technologies, cat.no. 10437028)
 - 1% penicillin-streptomycin (Fisher Scientific, cat. no. MT30002CI)
4. TCL buffer (Quiagen, cat. no. 1031576)
5. cold-storage adhesive sealing foil (VWR, cat. no. 89049-034)

3500 U-2 OS cells per well were plated in 384-well plates with 50 μ L culture medium. After 24 h of incubation at 37°C, compounds were added. Cells were treated for 6 h at 37°C before 40 μ L of medium was removed and 30 μ L TCL buffer added to lyse the cells. Plates were sealed with sterile sealing foil and, after 30 min incubation at room temperature (RT), stored at -80°C.

Gene-expression: sample preparation and measurement

We closely followed the protocol published by Peck et al. (13) Differences from the published materials and methods are summarized below. A detailed protocol follows.

1. Luminex microspheres: we used MagPlex instead of COOH
2. bead coupling preparation: we used a different volume of beads and wash solutions
3. probe hybridization: we introduced a ramp-down of annealing temperatures
4. polymerase: we used HotStarTaq Plus instead of HotStarTaq
5. PCR cycling conditions were different (29 cycles, 1min step times)
6. to measure all transcripts, we used 2 different bead mixes per sample during detection; furthermore, a different volume of each mix was used
7. bead/amplicon hybridization time: increased from 1 h to 16 h – 20 h

8. we introduced bead washes before and after streptavidin-phycoerythrin addition during detection, including new wash solutions
9. Luminex detection instrument: we used FlexMap 3D instead of Luminex 100

General Notes

All liquid transfers were automated on the Agilent Bravo Liquid Handling Platform. Between each step of the LMA protocol, unreacted products were removed by inverting the reaction plate onto a laboratory towel and centrifuging at 1000 g for 1 min. All non-room-temperature incubations took place on a Thermo Electron MBS 384 Satellite Thermal Cycler.

Luminex microsphere (bead) preparation

Materials:

1. Luminex xMAP MagPlex microspheres
2. bead binding buffer
 - 0.1 M 2-(N-morpholino)ethansulfonic acid (pH 4.5)
3. EDC solution
 - 10 mg/mL 1-ethyl-3-(3-dimethylaminopropyl)carbodiimide hydrochloride in water.
4. 0.02% Tween
5. 0.1% sodium dodecyl sulfate
6. TE (pH8)
 - 10 mM Tris-HCl (pH 8.0)
 - 1 mM EDTA

Luminex xMAP MagPlex microspheres were coupled to anti-barcode capture oligonucleotides. 490 distinct microsphere species were aliquoted into 800 μ L round-bottom deep well 96 plates, approximately 12.5×10^6 microspheres per well. Beads were pulled down by centrifugation and magnetic separation, storage buffer was removed, and beads were re-suspended in 130 μ L binding buffer. 500 pmol of capture probe was added to each microsphere well, such that each microsphere species well received a different probe. 5 μ L of a freshly prepared EDC solution was added, and the reactions were incubated for 30 min. EDC addition was repeated a second time. Microspheres were then captured by magnetic pull-down and washed successively in 500 μ L of Coupling 0.02% Tween, 0.1% sodium dodecyl sulfate, and TE (pH 8). Coupled microspheres were re-suspended in TE (pH 8) and pooled to a final concentration of 50,000 microspheres/ μ L. This pool constituted the first coupled microsphere set, referred to as dp52.

This process was repeated, such that the same 490 microsphere species were coupled to a different set of capture oligonucleotides, forming the second coupled microsphere set dp53.

Finally, 10 microsphere species were coupled to 80 different capture oligonucleotides, 8 oligonucleotides per microsphere species, to form a coupled microsphere pool assaying 10 invariant meta-genes.

Ligation Mediated Amplification

RNA extraction

Materials:

1. Turbocapture 384 mRNA kit (Qiagen, cat. no. 72271)

Frozen lysate was thawed for 1 h at room temperature. 20 μ L of lysate was transferred to a 384-well oligo-dT capture plate, and incubated at room temperature for 1h. During this incubation, mRNA was immobilized to the plate via binding of the poly-A tail.

cDNA Generation

Materials:

1. M-MLV Reverse Transcriptase kit (Promega, cat. no. M1705)
2. 100mM dNTP set (Invitrogen, cat. no. 10297018)

cDNA was generated from immobilized mRNA via reverse transcription. A 5 μ L M-MLV reaction mix was added to the reaction plate and incubated at 37°C for 1.5 h.

Probe Hybridization

1. pool of custom up- and down-stream probes
2. Taq DNA Ligase Reaction Buffer (NEB, cat. no. B0208S), used to prepare probe-pool working dilution

Custom up- and down-stream probes were hybridized to the cDNA. Upstream probes contained 20 nt of gene-specific sequence, a 24 nt FlexMap barcode, and the T7 priming site. Down-stream probes contained 20 nt of gene-specific sequence (designed to bind adjacent to the upstream probe) and the T3 priming site. Hybridization consisted of a 5 min 95°C denature followed by an annealing ramp-down from 70°C to 40°C, 12 min per degree. The reaction was held at 4°C overnight.

Probe Ligation

Materials:

- Taq DNA ligase kit (NEB, cat. no. M0208L)

Bound probes were ligated via a 5 μ L Taq DNA ligase reaction, incubated at 45°C for 1 h, followed by 65°C for 10 min.

PCR Amplification

Materials:

1. HotStarTaq Plus DNA polymerase kit (Qiagen, cat. no. 203603)
2. 100mM dNTP set (Invitrogen, cat. no. 10297018)

Ligated probes form a template competent for PCR using T3 and T7 universal primers. The T7 primer was biotinylated. A 15 μ L HotStarTaq Plus reaction mix was added to the plate, and the following PCR program performed:

- a. initial denature: 15 min @ 92°C
- b. 29 amplification cycles: 1 min @ 92°C – 1 min @ 60°C – 1 min @ 72°C
- c. final extension: 5 min @ 72°C

Hybridization and Detection

Microsphere Hybridization

Materials:

1. dp52 coupled bead set
2. dp53 coupled bead set
3. invariant-gene bead set
4. 1.5x TMAC hybridization solution
 - 4.5 M tetramethylammonium-chloride
 - 0.15% N-lauryl sarcosine
 - 75 mM Tris-HCl (pH 8)
 - 6 mM EDTA

Dilutions of each coupled flexmap microsphere set dp52 and dp53 were prepared in 1.5x TMAC hybridization solution, such that each reaction ultimately contained about 200 microspheres of each species. Additionally, “invariant-gene” microspheres were added to each dilution at a similar concentration. Invariant genes were genes selected to show relatively stable expression levels (coefficient of variation < 10%) across a large number of distinct reference samples. Eight invariant genes were selected at each of 10 expression levels. For each expression level, all 8 invariant genes were combined on one bead species. 23 μ L of diluted microspheres are plated in 384. 5 μ L of amplified LMA product was added to a dp52 dilution well and another 5 μ L to a dp53 dilution well. Samples were arranged such that the dp52 and dp53 wells were found on the same plate. The

resulting detection plate therefore contained 192 samples assayed on both bead sets. The detection plate was denatured at 95°C for 2 min, and incubated at 45°C for 16 h – 20 h overnight.

Microsphere Detection

Materials:

1. 1x TMAC hybridization solution
 - 3 M tetramethylammonium-chloride
 - 0.1% N-lauryl sarcosine
 - 50 mM Tris-HCl (pH 8)
 - 4 mM EDTA
2. low-stringency wash buffer
 - 6x SSPE
 - 0.01% Tween-20
3. high-stringency wash buffer
 - 0.1x MES
 - 25 mM NaCl
 - 0.01% Tween-20
4. reporter mix
 - 3% streptavidin-phycoerythrin (Invitrogen, cat. no. S866) in 1x TMAC hybridization solution

Microspheres were captured in the detection plate by centrifugation at 1000 rpm for 1 min followed by magnetic pull-down. Microspheres were washed successively in low-stringency wash buffer and high-stringency wash buffer. 10 μ L of reporter mix were added to each sample. Samples were incubated at 45°C for 10 min to allow streptavidin-phycoerythrin to bind the biotinylated amplicons. Samples were then centrifuged, magnetically pulled down, and washed with low-stringency wash buffer and 3 times with 1X TMAC wash solution. Labeled and washed microspheres were analyzed using the Luminex FlexMap 3D detector.

Gene-expression assay: data processing

Raw fluorescence intensity curves were processed by a peak-detection algorithm to yield expression values for each transcript in a sample. For each sample, the binary logarithms of expression values were normalized based on 80 pre-determined “invariant genes”, *i.e.*, genes that show relatively stable expression levels (coefficient of variation < 10%) across a large number of distinct reference samples. Eight invariant genes were selected at each of 10 expression levels. A calibration curve was computed for each sample using the median expression of these invariant genes. Samples were then rescaled using a reference curve computed from a large collection of expression profiles and limited to the range [0, 15] (<http://lincscloud.org/how-data-were->

prepared/). Detailed descriptions of the data-collection and data-processing pipeline will be published separately by the NIH LINCS project, and are summarized online (<http://lincscloud.org/>).

Gene-expression array: data normalization and correction

For each plate, the distributions of per-well gene-expression levels were quantile normalized. (14) Plate medians for all transcripts were subtracted from each well profile. Positional effects for each gene were corrected using GeneData Screener Assay Analyzer. (15) Robust Z-scores were calculated by dividing the resulting values by 1.4826 * plate median absolute deviation (MAD). We then calculated Stouffer's Z-score (16) to combine replicates into the final profiles for each compound.

Multiplexed cytological imaging assay

We followed the protocol published by Gustafsdottir et al. (17) Briefly, we seeded 1,500-2,000 U-2 OS cells (ATCC, cat. no. HTB-96) per well in 384-well clear-bottom imaging plates. After 24h of incubation at 37°C, compounds were added to the cells, followed by another 48h of incubation. Treatments were carried out in quadruplicates. We then stained six different cell compartments and organelles with fluorescent dyes: nucleus (Hoechst 33342), endoplasmic reticulum (concanavalin A/AlexaFluor488 conjugate), nucleoli (SYTO 14 green fluorescent nucleic acid stain), Golgi apparatus, and plasma membrane (wheat germ agglutinin/AlexaFluor594 conjugate, WGA), F-actin (phalloidin/AlexaFluor594 conjugate) and mitochondria (MitoTracker Deep Red). WGA and Mitotracker were added to living cells. The remaining stains were carried out after cell fixation with 16% paraformaldehyde. Images were captured in 5 fluorescent channels from 9 sites per well (20× magnification). We used the CellProfiler image-analysis software to calculate morphological features for each cell. (17)

Multiplex cytological imaging assay: materials

1. U-2 OS cells (ATCC, cat. no. HTB-96)
2. Aurora 384-well black/clear bottom plates, imaging quality (Brooks, cat. no. 1022-11330)
3. culture medium
 - DMEM (Fisher Scientific, cat.no. MT10017CV)
 - 10%FBS (Life Technologies, cat.no. 10437028)
 - 1% penicillin-streptomycin (Fisher Scientific, cat. no. MT30002CI)
4. Mitotracker Deep Red (Invitrogen, cat. no. M22426)
5. wheat germ agglutinin Alexa 594 conjugate (Invitrogen, cat.no. W11262)
6. paraformaldehyde 16%, methanol free (Electron Microscopy Sciences, cat. no. 15710-S)
7. Hank's Balanced Salt Solution, HBSS (Invitrogen, cat. no. 14065-056)
8. Triton X-100 (Sigma, cat. no. T8787)
9. phalloidin 594 (Invitrogen, cat. no. A12381)
10. concavalin A 488 (Invitrogen, cat. no. C11252)

11. Hoechst 33342 (Invitrogen, cat. no. H3570)
12. SYTO 14 green fluorescent nucleic acid stain (Invitrogen, cat.no. S7576)
13. sodium bicarbonate (HyClone, cat. no. SH30033.01)
14. methanol (BDH, cat. no. 67-56-1)
15. bovine serum albumin
16. REMP blue thermo heat seal (REMP/Nexus Biosystems, cat. no. 1800336)
17. ImageXpress Micro (Molecular Devices)

Multiplex cytological imaging assay: assay protocol

U-2 OS cells were plated at a density of 1500-2000 cells per well with 50 μ L culture medium. After 24 h incubation at 37°C, compounds were added. Cells were treated for 48 h at 37°C. A 1 mM solution of Mitotracker in DMSO and a 1 mg/mL solution of wheat germ agglutinin (WGA) in distilled water were used to prepare a staining solution of 500nM Mitotracker and 60 μ g/mL WGA in pre-warmed medium. After removal of 40 μ L of media from the cells, 30 μ L of the staining solution were added to each well and incubated for 30 min at 37°C. Cells were fixed for 20 min at RT with 10 μ L paraformaldehyde and afterwards washed once with 70 μ L HBSS. To permeabilize cells, 30 μ L of a 0.1% solution of Triton X-100 in 1x HBSS were added, incubated for 10-20 min, and washed two times with 70 μ L 1xHBSS. Concanavalin A was dissolved to 1 mg/mL in 0.1 M sodium bicarbonate solution. Phalloidin was dissolved in 1.5 mL methanol per vial. Staining mix was prepared from 0.025 μ L phalloidin/ μ L, 100 μ g/mL Concanavalin, 5 μ g/mL Hoechst, and 3 μ M SYTO staining solution in 1x HBSS 1% BSA. Aliquots of 30 μ L staining mix were added to each well and incubated for 30 min. After staining, cells were washed three times with 70 μ L 1xHBSS without final aspiration. Plates were thermally sealed at 171°C (4 seconds).

Multiplex cytological imaging assay: image capture

We captured images on an ImageXpress Micro epifluorescent microscope. We recorded 9 sites per well at 20x magnification in 5 fluorescent channels, DAPI (387/447 nm), GFP (472/520 nm), Cy3 (531/593 nm), TexasRed (562/642 nm), Cy5 (628/692 nm). The first site of each well was used for laser-based auto-focus in the DAPI channel.

Multiplex cytological imaging assay: image analysis and data processing

CellProfiler (18) software version 2.0.9925 was used to locate and segment cells and measure morphological features for each cell. We used pipelines described and provided by Gustafsdottir *et al.* (17) to correct for uneven illumination and segment cells into nuclei and cytoplasm. Size, shape, texture, intensity statistics, and local density were measured for nuclei, cytoplasm, and entire cells. (17) Cell-morphology features were normalized by linearly scaling the 1st and 99th percentiles of

the DMSO-control distributions to 0 and 1, respectively. Plate medians were subtracted from each profile and positional effects corrected with GeneData Screener Assay Analyzer. (15)

HTS assay information

HTS assay results were assembled from an internal database at the Broad Institute. However, for the majority of assays, results have been deposited in public databases (ChemBank and PubChem/BARD; Datasets S1 and S2). We distinguished between screening projects, assays, and individual assay measurements with screening projects representing the highest level of organization in the respective database. For ChemBank, assays were defined as all experiments in a screening project that share the same detection method. Assay measurements were defined as all experiments in an assay that share the same experimental conditions and time point.

For PubChem/BARD and internal screening projects, assays were defined as annotated by the experimenter who submitted the screen. Assay measurements were defined as all direct measurements and calculated values that convey information different from the direct measurements (e.g., a ratio of two direct measurements).

Compound activity for profiling assays and activity score

We used the multidimensional perturbation value (mp-value) as described by Hutz et al. (19) to determine compound activity in profiling screens. The profiles for all replicates of a compound within a batch were combined into a matrix with the profiles from the corresponding negative DMSO-control wells in the same batch such that rows represent wells and columns represent profiling features. The matrix, generated for each compound separately, was then standardized by first calculating a z-score across rows and then columns. Principal component analysis was performed on the standardized matrices and the first n principal components that sum up to a variance of 0.9 were retained. Each of these n principal components was weighted by the percentage of variance it explains (by multiplying the matrix with the vector of variances) to obtain the normalized matrix P .

P was split into treatment and control rows and for each of the parts a covariance matrix was calculated. Each of two covariance matrices (treatment and control) was weighted by the number of samples in each group. The sum of the resulting matrices was used to calculate the Mahalanobis distance between treatment and control samples.

To calculate a p-value based on the Mahalanobis distance, we performed an empirical test with 1000 permutations. Each time the treatment/control labels were randomly assigned and the distance recalculated to estimate a distribution of distances. A p-value was then calculated as the fraction of distance values that are equal to or larger than the real distance value. Compounds with a p-value lower than 0.05 were considered active.

We calculated a normalized “activity score” to use the calculated Mahalanobis distance as an additional constraint for activity (as suggested by Hutz et al. (19)). We scaled the distribution of distances for all compounds linearly such that the [0.2, 99.8]-percentile range mapped to [0, 1].

Promiscuity probability

The probability of a compound showing promiscuous HTS assay activity (or ‘cross-reactivity’) was calculated according to Dančík *et al.* (20) Based on past screening results, we calculated the mean (0.13) and standard deviation (0.012) of hit frequencies for all compounds. These values were used to determine parameters α and β of a beta-distribution:

$$\mu = \frac{\alpha}{\alpha + \beta}$$

$$\sigma^2 = \alpha\beta(\alpha + \beta)^{-2}(\alpha + \beta + 1)^{-1}$$

For each compound, we determined the number of assays N in which it was tested, and the number of assays n in which it scored as a hit and calculated the probability of having a hit frequency θ higher than $\theta_0 = 0.25$ using the MATLAB function `betainc`,

$$P(\theta > \theta_0) = \text{betainc}(\theta_0, n + \alpha, N - n + \beta, 'upper').$$

Supporting Figures

Figure S1. Annotated bioactive compounds clustered based on MC profiles form groups with similar biological effects.

We hierarchically clustered all compounds of the MC hit set for which a common name was available based on their imaging profiles. We used complete linkage applied to correlation distance (1-Pearson coefficient). Compounds that do not have a neighbor closer than 0.2 correlation distance are omitted for clarity. Compound names are reported next to the dendrogram. Where known, the compound's primary biological effect or use is reported. If groups of compounds with related biological effects co-cluster, their common effect is summarized (indicated by a larger font size).

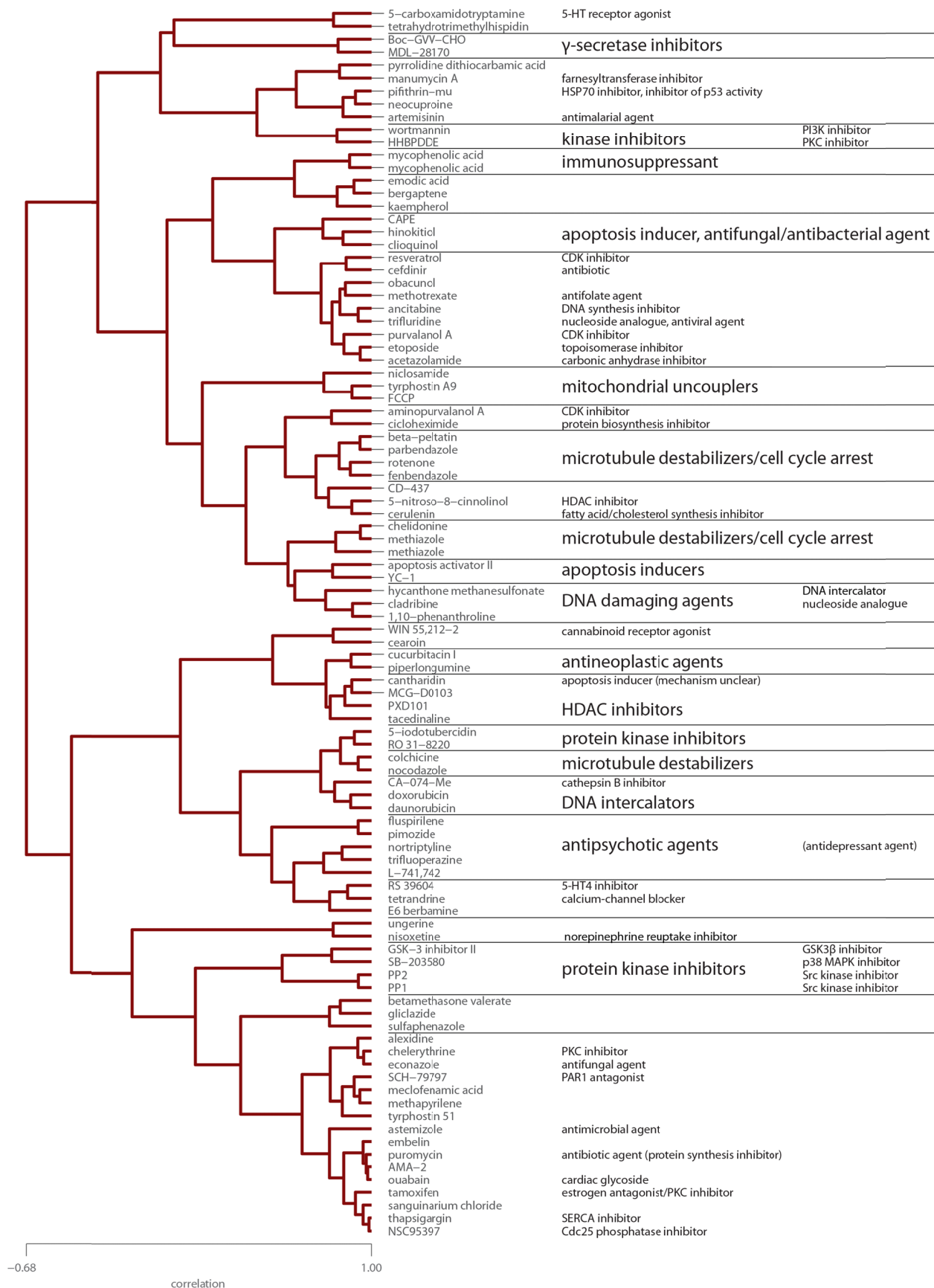


Figure S2. MC and GE profile diversity leads to HTS outcome diversity.

We compared the HTS outcome diversity for subsets of compounds selected from (a) the MC test collection and (b) the GE test collection. The subsets were selected to have diverse MC profiles, GE profiles, or chemical structures (CS), as indicated by the label for each curve. We compared the HTS performance diversity of sets selected based on MC or GE profile diversity or CS diversity to randomly selected compound sets of the same size (RND).

Diverse subset selection from the hit-sets was performed iteratively using a maximum dissimilarity strategy. The first compound in this process was selected randomly. We then iteratively added the compound to the growing list that had the most dissimilar MC profile (GE profile; CS) to the already selected ones. We monitored the change in HTS performance diversity throughout this selection process. HTS performance diversity was measured as the “true diversity” (see Methods). This measure penalizes redundancy and over-representation of individual profiles in a compound set. Therefore, adding a novel HTS profile to the set will increase diversity whereas adding a profile already contained in the set will decrease it. The maximum diversity (100%) is reached when an equal number of compounds represent each distinct assay profile in the respective hit set. (21) Effectively, this procedure provides a ranking of compounds by their contribution to the diversity of the entire set. Monitoring the HTS performance diversity provides a measure for the diversity of the top N diverse compounds, where N ranges from 1 to the size of the respective test collection. Because the first compound was selected randomly, the entire selection was repeated 500 times, each time with a different starting point (resulting in 500 distinct ranked lists). The average HTS performance diversity over these 500 rankings (+/- standard deviation, sd) is plotted for the top N compounds. The vertical line indicates the set size that achieved the maximum diversity across all of the selection methods. This set size was used for to generate the bar charts in Fig. 4b and 4c in the manuscript as well as Fig. S3.

(a) The diversity curves show that selection using MC profile diversity led to higher HTS outcome diversity than random selection and selection based on chemical structure diversity. Each selection method (MC, CS, RND) picked distinct profiles at first, leading to a steep increase in diversity near the top of the list. However, after many selections, random selection will choose profiles that are already in the set, indicated by a flattening of the diversity curve. Since there is no differential selection possible for the full set, all curves converge when the diversity of the full compound set is reached (23.9%; right end of the plot). However, selection based on the MC diversity rankings leads to a prolonged increase in HTS outcome diversity and hence reaches a higher level than random compound selection. This result indicates that MC profile diversity can inform the selection of a performance-diverse compound set for cell-based screens. Selection on chemical structure diversity performed worse than MC and even led to lower performance diversity than random selection. (b) Similar results are observed for the GE test collection, where diversity selection based on GE profiles outperforms RND and CS, leading to higher HTS performance diversity. Likely due to the lower numbers of compounds in the GE study, GE-profile-based selection led to a lower increase over random than MC.

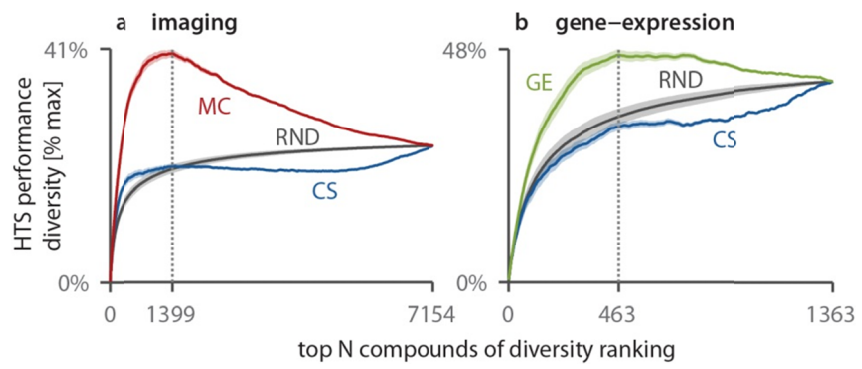


Figure S3. Assay-profile cluster coverage of different diversity selection methods.

We compared the number of distinct HTS assay profile clusters (groups of compounds with similar performance across HTS assays) that were covered by compound sets selected to have diverse MC profiles, GE profiles, or chemical structure (CS). We compared these to a baseline of randomly selected sets of the same size (RND). We clustered compounds based on similar HTS performance patterns using hierarchical clustering (see Methods for details). Diverse compound subsets were selected from (a) the MC test collection (1399 compounds; marked with a dashed line in Fig. S2a) and (b) the GE test collection (463 compounds; marked with a dashed line in Fig. S2b). The diversity subsets used here were identical to the ones used in Fig. 4 of the manuscript. Analogous to the results shown in Fig. 4b, 4c, and 5c of the manuscript, sets with diverse MC or GE profiles cover more HTS clusters than sets with diverse chemical structure or randomly selected sets. Likewise, selection of diverse GE profiles led to comparably smaller improvements of HTS cluster coverage over CS and RND (b) than selection of diverse MC profiles (a), likely due the lower number of compounds available for the GE study.

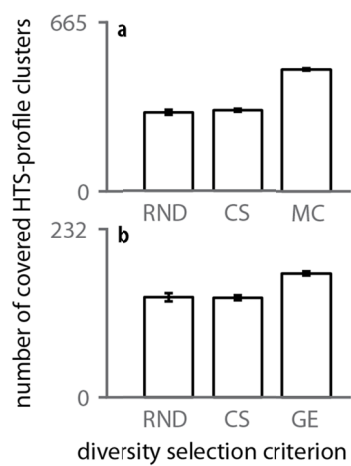


Figure S4. Annotated bioactive compounds clustered based on GE profiles form groups with similar biological effects.

We hierarchically clustered all compounds of the GE hit set for which a common name was available based on their gene-expression profiles. We used complete linkage applied to correlation distance (1-Pearson coefficient). Compounds that do not have a neighbor closer than 0.35 correlation distance are omitted for clarity. Compound names are reported next to the dendrogram. Where known, the compound's primary biological effect or use is reported. If groups of compounds with related biological effects co-cluster their common effect is summarized (indicated by a larger font size). Compounds that are present multiple times are positive controls included in multiple instances throughout the experiment.

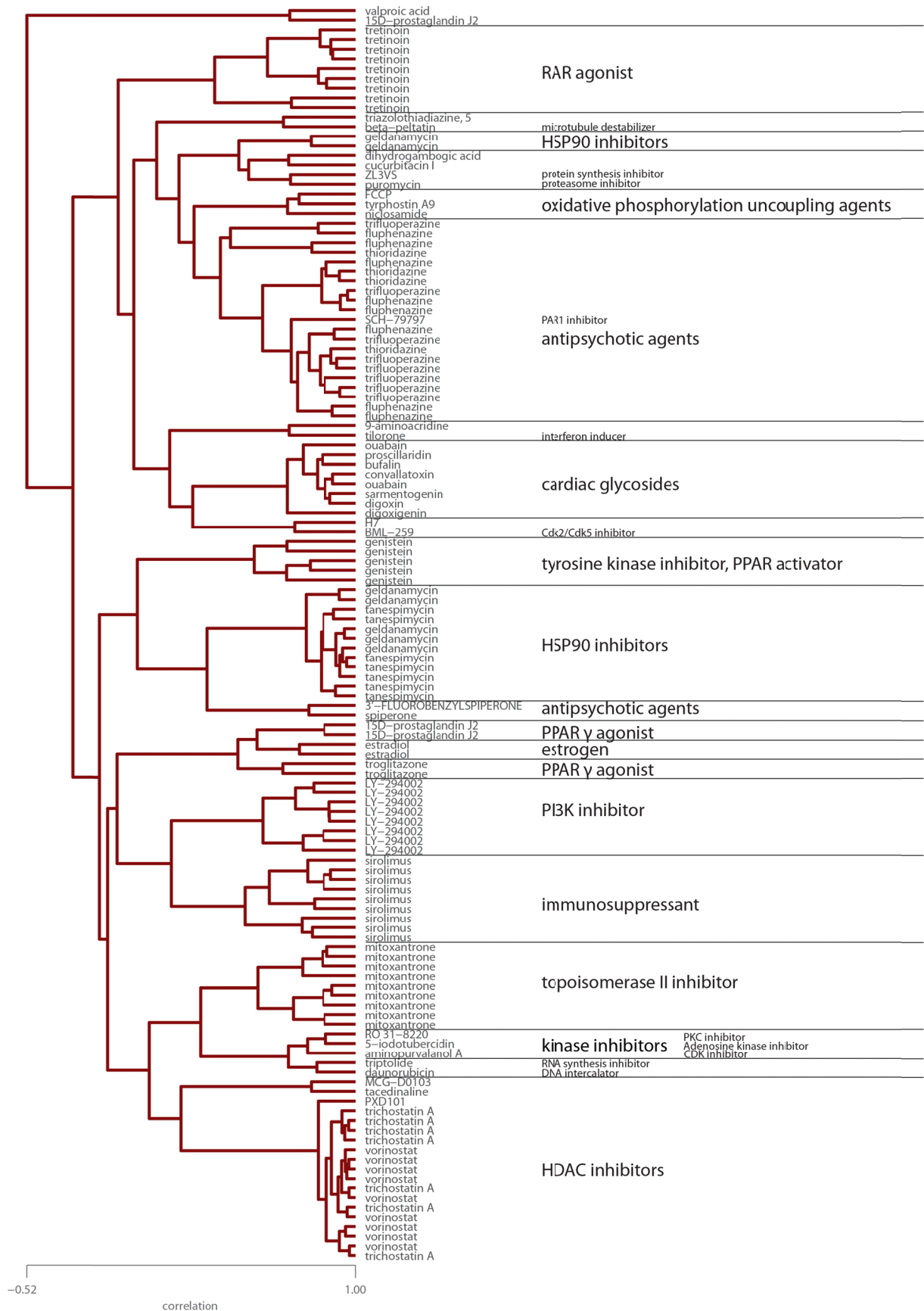


Figure S5. Compounds active for both MC and GE are more promiscuous than hits in either assay individually.

Cumulative distributions of promiscuity probability values (see “Promiscuity probability” in Supporting Methods for details) are shown for compounds active in the MC assay, the GE assay, or both assays. The right-shift of the red curve (hits in both MC and GE assays) compared to the black (hits in GE assay) and blue curves (hits in MC assay) indicate that the set of compounds that were hits in both assays was enriched for promiscuous compounds, *i.e.*, compounds that are active in many HTS assays, likely due to unspecific activity (*e.g.*, cytotoxicity).

The median promiscuity probability (pp) is significantly higher for the intersection of both assays [median(pp) = 0.33%] than for MC [median(pp) = 0.15%; $p = 7.6 \times 10^{-14}$] or GE alone [median(pp) = 0.15%; $p = 5.7 \times 10^{-7}$].

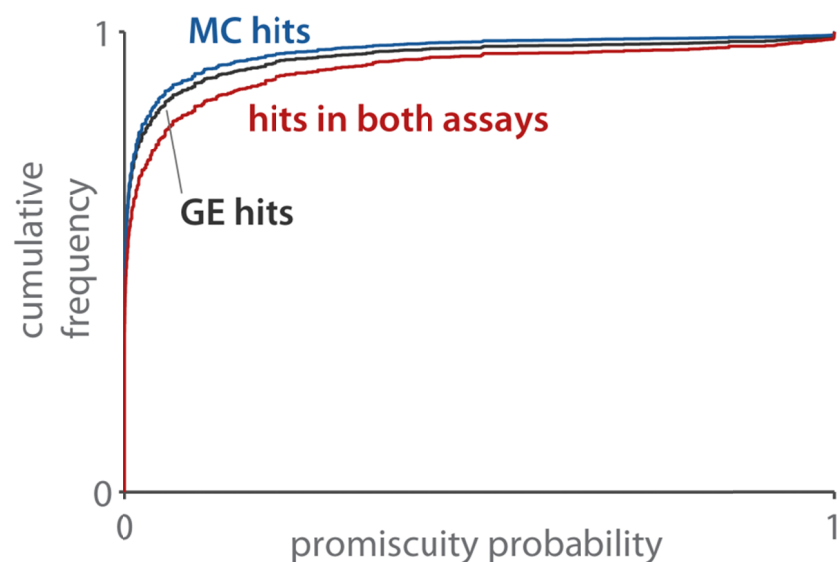


Figure S6. MC leads to slightly higher HTS performance diversity when compared to GE on the overlap between the MC and GE test collections. We applied maximum dissimilarity diversity selection to the overlap between the MC and GE test collections to directly compare the level of HTS performance diversity achieved by diversity selection based on MC and GE profiles on the same compound set (see Fig. S2 for a detailed description of maximum dissimilarity diversity selection).

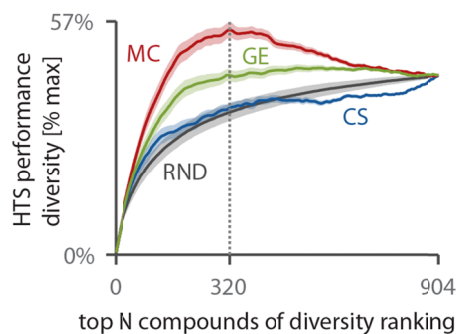


Figure S7. Assay-profile cluster coverage of different diversity-selection methods - calculated on the overlap of MC and GE test collections. The bar chart shows the number of HTS assay profile clusters covered by different selection methods (RND, random; CS, chemical structure; MC, imaging profiles; GE, gene-expression profiles) for a set size of 320 compounds, which achieved the overall highest performance diversity for the intersection of test collections (indicated by the dashed line in Fig. S6).

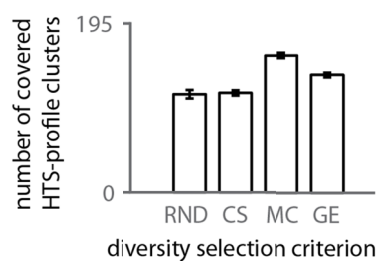


Table S1. Composition of profiling compound collection and hit sets.

	BIO			DOS			POS			all		
	N	hits	hit rate	n	hits	hit rate	n	hits	hit rate	n	hits	hit rate
MC	12431	8490	68.3	17805	6594	37.0	-	-	-	30236	15084	49.9
GE	4199	1639	39.0	17553	1924	11.0	29	28	96.6	21781	3591	16.5
union	12606	9009	71.5	19164	7606	39.7	-	-	-	31770	16615	52.3

Table S2. Detection method used in assay measurements.

detection method	frequency	frequency [%]
fluorescence	290	56.64%
luminescence	150	29.30%
cytoblot	28	5.47%
absorbtion	4	0.78%
qPCR	2	0.39%
alphaLISA	1	0.20%
other	37	7.23%

Table S3. Assay kits used in assay measurements.

assay kit	frequency	frequency [%]
CellTiter-Glo	100	19.53%
Resazurin	85	16.60%
Calcein	44	8.59%
JC-1	33	6.45%
Reporter	29	5.66%
Bromodeoxyuridine	20	3.91%
NileRed	9	1.76%
AmplexRed	7	1.37%
DAPI	6	1.17%
Caspase-Glo	6	1.17%
OilRedO	5	0.98%
MTT	4	0.78%
other	164	32.03%

Table S4. Cells used in assay measurements.

cell type	frequency	frequency [%]
primary	142	27.73%
A549	67	13.09%
HEK293	15	2.93%
NIH/3T3	14	2.73%
U2OS	14	2.73%
HeLa	14	2.73%
H1299	13	2.54%
PC9	13	2.54%
LN229	13	2.54%
hES	12	2.34%
MEF	7	1.37%
Alpha-TC-1;Beta-TC-3	6	1.17%
mES	5	0.98%
C2C12	5	0.98%
HTB-65	4	0.78%
786-O	4	0.78%
HUVEC	4	0.78%
A498	4	0.78%
MCH58	4	0.78%
HepG2	4	0.78%
worm	3	0.59%
DLD1	3	0.59%
MM1S	3	0.59%
RKO	3	0.59%
HT22	3	0.59%
RPMI8826	3	0.59%
Huh7	3	0.59%
SK-MEL-5	3	0.59%
HMLE	3	0.59%
MEF-1	2	0.39%
INS-1E	2	0.39%
J774A.1	2	0.39%
mPASC	2	0.39%
U251	2	0.39%
BHK	2	0.39%
KoptK1	2	0.39%
Min6	2	0.39%
L6	2	0.39%
PC12	2	0.39%
H4	1	0.20%
D54	1	0.20%
BHK-21	1	0.20%
CEM21;HeLa	1	0.20%
BJ	1	0.20%
CRL-5865	1	0.20%
DKS8	1	0.20%
BG1	1	0.20%
LNCaP	1	0.20%
COS-7	1	0.20%
CCL-185	1	0.20%
BJAB	1	0.20%
Hct116	1	0.20%
HKE3	1	0.20%
other	87	16.99%

Table S5. MC and GE have significantly overlapping yet distinct hit sets.

Numbers represent compounds tested in both experiments. The null hypothesis of MC and GE hit sets being independent can be rejected for the set of all compounds and the DOS collection based on *p*-values calculated with Fisher's exact test. The BIO set does not show significant overlap because both MC and GE identify many of the 4053 compound as hits. Therefore, a large overlap is expected.

	n	hits MC	hits GE	overlap	<i>p</i>-value
BIO	4053	3018	1557	1148	0.81
DOS	16194	6026	1837	912	1.13E-31
all	20247	9044	3394	2060	3.70E-94

Table S6. Compounds active in both MC and GE assays are often promiscuous

Shown are compounds active in both MC and GE with a promiscuity probability > 0.5 (see “Promiscuity probability” and Dančík *et al.* (20)) for which common names were available.

compound_name	PubChem_CID
3'-fluorobenzylpiperone	3248000
5-iodotubercidin	1830
5-nitroso-8-cinnolinol	44483284
AMA-2	160020
BADGE	2286
CD-437	135411
dihydroergocristine	11072143
FCCP	3330
GR 55562	128018
H7	3542
L-741,742	133008
LE-135	10410894
LY-294002	3973
MCG-D0103	9865515
NSC95397	262093
PXD101	6918638
R(+)-6-bromo-APB	10452020
R(-)-2,10,11-trihydroxy-N-propyl-noraporphine	6603798
RO 31-8220	5083
SB-415286	4210951
SCH-79797	4259181
ZL3VS	5497183
aminoacridine	7019
aminopurvalanol A	6604931
apomorphine hydrochloride	6005
bepriidil	2351
beta-peltatin	92122
calcimycin	40486
cantharidin	2545
cicloheximide	6197
colchicine	6167
cucurbitacin I	44483311
curcumin	969516
daunorubicin	30323
emetine	10219
etoposide	36462
fenbendazole	3334
hinokitiol	3611
hycanthone methanesulfonate	3634
mefloquine	4046
metergoline	28693
methiazole	6604471
mycophenolic acid	446541

niclosamide	4477
nocodazole	4122
ouabain	439501
parbendazole	26596
phorbol myristate acetate	27924
pimozide	16362
puromycin	2724365
sanguinarium chloride	5154
suloctidil	657255
tacedinaline	2746
tetrandrine	73078
thapsigargin	446378
trifluoperazine	5566
trifluridine	6708818
tyrphostin A9	5614
tyrphostin AG 1296	2049
tyrphostin AG-1478	2051
tyrphostin AG879	6809654

Supporting Datasets

Dataset S1. Listing of assays and assay measurements published in ChemBank.

ChemBank experiment IDs and links are listed for each assay (provided as a separate Excel file).

Dataset S2. Listing of assay measurements published in PubChem and BARD.

PubChem Assay IDs (AIDs) and BARD Assay Definition IDs (ADIDs) are listed for each assay (provided as a separate Excel file).

Supporting References

1. Kelly AR, *et al.* (2009) Accessing skeletal diversity using catalyst control: formation of n and $n + 1$ macrocyclic triazole rings. *Org. Lett.* 11(11):2257-2260.
2. Marcaurelle LA, *et al.* (2010) An aldol-based build/couple/pair strategy for the synthesis of medium- and large-sized rings: discovery of macrocyclic histone deacetylase inhibitors. *J. Am. Chem. Soc.* 132(47):16962-16976.
3. Gerard B, *et al.* (2011) Synthesis of a stereochemically diverse library of medium-sized lactams and sultams via S(N)Ar cycloetherification. *ACS Comb. Sci.* 13(4):365-374.
4. Fitzgerald ME, *et al.* (2012) Build/couple/pair strategy for the synthesis of stereochemically diverse macrolactams via head-to-tail cyclization. *ACS Comb. Sci.* 14(2):89-96.
5. Comer E, *et al.* (2011) Fragment-based domain shuffling approach for the synthesis of pyran-based macrocycles. *Proc. Natl. Acad. Sci. U S A* 108(17):6751-6756.
6. Gerard B, *et al.* (2011) Large-scale synthesis of all stereoisomers of a 2,3-unsaturated C-glycoside scaffold. *J. Org. Chem.* 76(6):1898-1901.
7. Gerard B, *et al.* (2012) Application of a Catalytic Asymmetric Povarov Reaction using Chiral Ureas to the Synthesis of a Tetrahydroquinoline Library. *ACS Comb. Sci.*
8. Gerard B, *et al.* (2013) Synthesis of stereochemically and skeletally diverse fused ring systems from functionalized C-glycosides. *J. Org. Chem.* 78(11):5160-5171.
9. Nielsen TE & Schreiber SL (2008) Towards the optimal screening collection: a synthesis strategy. *Angew. Chem. Int. Ed. Engl.* 47(1):48-56.
10. Burke MD & Schreiber SL (2004) A planning strategy for diversity-oriented synthesis. *Angew. Chem. Int. Ed. Engl.* 43(1):46-58.
11. Rogers DJ & Tanimoto TT (1960) A Computer Program for Classifying Plants. *Science* 132(3434):1115-1118.
12. Rogers D & Hahn M (2010) Extended-connectivity fingerprints. *J. Chem. Inf. Model.* 50(5):742-754.
13. Peck D, *et al.* (2006) A method for high-throughput gene expression signature analysis. *Genome Biol.* 7(7):R61.
14. Bolstad BM, Irizarry RA, Astrand M, & Speed TP (2003) A comparison of normalization methods for high density oligonucleotide array data based on variance and bias. *Bioinformatics* 19(2):185-193.
15. Genedata Screener Assay Analyzer (Genedata, Basel, Switzerland), 10 (2013).
16. Stouffer SA, Suchman EA, DeVinney LC, Star SA, & Williams RMJ (1949) *Studies in Social Psychology in World War II: The American Soldier* (Princeton University Press, Princeton).
17. Gustafsdottir SM, *et al.* (2013) Multiplex cytological profiling assay to measure diverse cellular states. *PLoS One* 8(12):e80999.
18. Kamentsky L, *et al.* (2011) Improved structure, function and compatibility for CellProfiler: modular high-throughput image analysis software. *Bioinformatics* 27(8):1179-1180.
19. Hutz JE, *et al.* (2013) The multidimensional perturbation value: a single metric to measure similarity and activity of treatments in high-throughput multidimensional screens. *J. Biomol. Screen.* 18(4):367-377.
20. Dancik V, *et al.* (2014) Connecting Small Molecules with Similar Assay Performance Profiles Leads to New Biological Hypotheses. *J. Biomol. Screen.* 19(5):771-781.
21. Clemons PA, *et al.* (2011) Quantifying structure and performance diversity for sets of small molecules comprising small-molecule screening collections. *Proc. Natl. Acad. Sci. U S A* 108(17):6817-6822.